JOURNAL OF APPLIED ELECTROCHEMISTRY 24 (1994) 981–988

Simultaneous underpotential deposition of lead and thallium on polycrystalline silver-III

S. BHARATHI, V. YEGNARAMAN, G. PRABHAKARA RAO*

Central Electrochemical Research Institute, Karaikudi-623 006, India

Received 29 May 1993; revised 2 February 1994

Simultaneous underpotential deposition of lead and thallium from a tartrate medium on a polycrystalline silver electrode is reported. Results of cyclic voltammetric investigations of the effects of concentration and sweep rate on the codeposition behaviour are discussed. Further investigations of the codeposition behaviour through voltammetric experiments using programmed potential inputs are described and discussed in terms of formation of a two-dimensional alloy. Finally, the validity of the existing models of electrochemical phase formation has been investigated under the codeposition conditions.

Nomenclature

I_{pn}	nondimensional peak current
E_{pn}	nondimensional peak potential
$\Delta E_{\frac{1}{2}n}$	nondimensional half-peak width
Q_M	charge due to UPD coverage of metal 'M' ($\mu C\,cm^{-2}$)
t_d	holding time (s)
v	sweep rate ($V\,s^{-1}$)
E	potential (V)
β	instantaneous nucleation growth rate constant

1. Introduction

Underpotential deposition (UPD) of a metal over a foreign metallic substrate is an important area of study, due to its possible application in electrocatalysis and modification of electrodes [1–5]. It can also provide insight into the phenomenon of electrocrystallization associated with the electrodeposition of metals [6, 7]. However, attempts to codeposit UPDs of two metals have been scarce [8–10]. Such studies of codeposition, wherein two metals in their UPD state are simultaneously deposited on a single metallic substrate, provides interesting information on surface processes such as (i) adsorbate–substrate interaction in presence of another adsorbate and (ii) adsorbate–adsorbate interaction. Further, this codeposition approach may advantageously be employed to study the formation and characterization of two-dimensional alloys. It can also offer scope for designing a bifunctional catalyst through the incorporation of two different metals on a suitable substrate. The fact, that codepositing UPDs has not received much attention may be due to the interference caused by the bulk deposition of the more electropositive metal with UPD of the other. Recently, mixed UPDs of two metals (Ag and Pb or Tl) on a gold single crystal electrode has been reported by Juttner *et al.* [11–13] who adopted a sequential deposition approach in which silver was initially deposited in submono, mono or multilayer amounts at fixed under and overpotentials followed by UPD of lead. STM studies showed that silver is epitaxially deposited on the gold surface. At low degrees of coverage (less than or just one monolayer) the voltammograms exhibited UPD peaks characteristic of Ag/Pb and Au/Pb while at high silver coverages (just or greater than two monolayers) a UPD peak corresponding to Ag/Pb alone was formed.

An entirely different method of obtaining mixed UPDs of two metals relies on simultaneous deposition of the two UPDs from the solution containing both the metals ions. This approach involves shifting the UPD potentials of the two metals to within a narrow potential window wherein the bulk deposition does not occur. Pb(II) forms more stable complexes with ligands than Tl(I). Hence, in the presence of complexing anions, the lead UPD potential may shift closer to the thallium UPD potential. The use of complexing anions, along with the judicious choice of the cation concentration, is expected to facilitate codeposition. Thus, by the introduction of a suitable complexing anion, codeposition has successfully been accomplished [14]. Investigations on lead and thallium UPDs on polycrystalline silver from citrate medium have proved this feasibility [14–16] and have revealed that, in the complexing medium, (i) the UPD peak shifts cathodically and becomes sharper and (ii) the extent of peak shifts and reduction in half peakwidths increase with increase in complexing anion concentration. This tendency is marked in the case of lead UPD while it is marginal for thallium UPD. These observations prompted

* To whom correspondence should be addressed.

0021-891X © 1994 Chapman & Hall

further work to extend the codeposition studies to other complexing anions for obtaining information on the possibility of mixed UPDs in such media together with their kinetics and growth mechanism. Experimental results obtained on the codeposition in tartrate and EDTA media are reported in this communication.

2. Experimental details

An all glass three electrode cell described elsewhere [16] was employed. The working electrode was a polycrystalline silver disc of 0.378 cm^2. A platinum foil and a normal calomel electrode (NCE) served as counter and reference electrodes respectively. All potentials are referred to NCE. The working electrode was polished using alumina slurry (particle size 0.05 μm) and subsequently cleaned under sonication. A Wenking Potentioscan (Model POS 73) along with a Rikadenki *XY-t* Recorder (Model RW 201T) was employed for recording cyclic voltammograms (c.v.). For experiments with specially programmed potential inputs, a digital potentiostat (EG&G PAR Model 273) was employed. All chemicals were of analytical grade and were used without further purification. Prior to experiments, solutions were purged with pure nitrogen for 1 h. Sodium potassium tartrate solution (0.1 M) containing 0.01 M H_2SO_4 was employed as the electrolyte. Single metal UPDs, as well as mixed UPDs, were obtained from the above media containing appropriate concentrations of the metal/mixture of metal ions.

3. Results and discussion

3.1. *UPD behaviour of Pb and Tl from single salt solutions*

The individual behaviour of lead and thallium from the respective single salt solution in tartrate revealed characteristic UPD deposition and dissolution peaks for the metal (Fig. 1). The UPD deposition potentials of lead and thallium occur at −0.46 V (curve (a)) and −0.59 V (curve (b)), respectively (cf. −0.55 and −0.63 V, respectively, in citrate [16]). The underpotential shifts (difference between bulk and UPD deposition potentials) obtained individually for lead and thallium in this medium are 0.17 and 0.25 V, respectively, and are in good agreement with those predicted by Kolb's relation [17]. The data also indicate that, in tartrate, the lead UPD peak becomes sharper and shifts cathodically with respect to that observed in perchlorate medium. The extents of peak shift and the reduction in half-peakwidth increase with increasing tartrate concentration, as earlier observed in citrate [16]. The thallium UPD, however, was noted to respond less markedly under similar conditions, akin to its behaviour in citrate. In this context, it is pertinent to recall, that from a non-complexing perchlorate medium, a second thallium monolayer on silver has been observed [18]

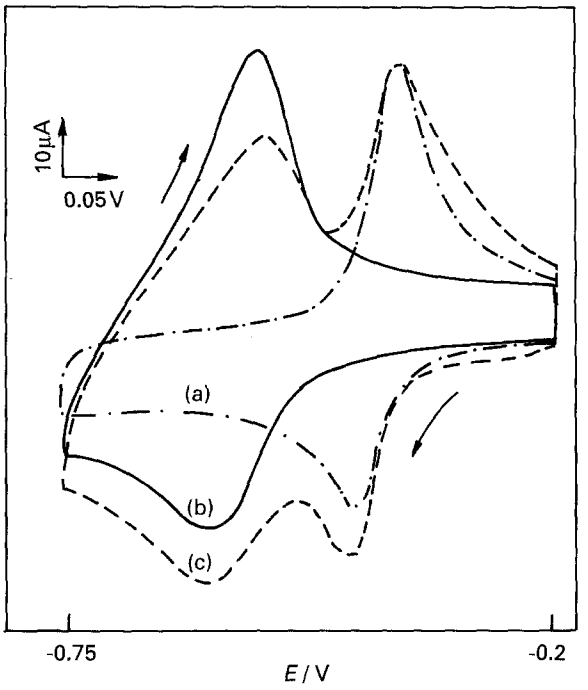

Fig. 1. CV response of polycrystalline silver at 0.1 Vs^{-1} from solution containing (a) 5×10^{-5} M of Pb(II), (b) 10^{-4} M of Tl(I), (c) 5×10^{-5} M of Pb(II) and 10^{-4} M of Tl(I).

while only a single thallium monolayer results from the presently studied complexing medium.

Interestingly, in EDTA medium [19], the cathodic shift for the lead UPD peak is larger than that observed in citrate and tartrate media. Further, the separation between the UPD deposition and dissolution peaks (ΔE_p) in EDTA is far higher ($\sim$ 0.15 V) than that obtained in citrate or tartrate ($\sim$ 0.03 V). Consequently, the deposition sequence of lead and thallium UPDs during codeposition is found to be reversed; i.e. thallium UPD, in EDTA, precedes lead UPD while in citrate and tartrate media it follows lead UPD. The observed linear variation [19] between the logarithm of the stability constant and the monolayer equilibrium potential (midpoint of the UPD deposition and dissolution potentials) indicates the relationship between the UPD behaviour of the metal and the stability of the corresponding complexes, as noted recently in the case of copper UPD on platinum [20]. The surface coverages (Q_M) for lead and thallium UPDs studied individually from the tartrate medium depend on the metal ion concentration. The data presented in Table 1 reveal submonolayer coverages for both lead and thallium at lower concentrations and near

Table 1. Effect of Pb(II)/Tl(I) concentration in tartrate (0.1 M sodium potassium tartrate and +0.01 M sulphuric acid) medium on monolayer coverage of the individual Pb/Tl UPD

Concentration Pb(II)/Tl(I)/mM	$Q_{Pb}/\mu C\,cm^{-2}$	$Q_{Tl}/\mu C\,cm^{-2}$
0.05	125	90
0.1	275	108
1.0	330	200

full monolayer coverage at concentrations greater than 0.1 mM (where Q_M reaches $350 \pm 20\,\mu C\,cm^{-2}$ for lead and $190 \pm 20\,\mu C\,cm^{-2}$ for thallium, respectively).

3.2. *Codeposition of lead and thallium UPDs*

3.2.1. Effect of concentration of Pb(II) and Tl(I). A c.v. describing the codeposition of lead and thallium UPDs from tartrate medium is also presented in Fig. 1 (curve (c)). It can be seen that the UPD potential region of lead and thallium can be swept without interference from the bulk deposition of either metal. Further, by comparison with c.v.'s obtained for individual lead and thallium UPDs (curves (a) and (b) in Fig. 1) the peaks at −0.46 and −0.59 V correspond to those of lead and thallium, respectively.

During codeposition, lead UPD (−0.46 V) precedes thallium UPD (−0.59 V). Hence the presence of lead UPD on silver substrate is expected to influence the thallium UPD behaviour. Experiments were carried out keeping Tl(I) constant at 0.1 mM and varying Pb(II) from 0.01 to 1 mM. At low concentration of lead (0.05 mM), thallium UPD is predominant, as indicated by the formation of its well defined peaks and the lead UPD is less marked by the presence of a small hump at −0.44 V. The absence of a well defined peak for lead UPD may be due to the low Pb(II). At high lead concentrations (0.5 mM), thallium UPD is completely masked by the lead UPD. In the intermediate concentrations, the UPDs corresponding to both lead and thallium are well marked and the lead UPD tends to predominate as its concentration is increased, resulting in lower coverage due to thallium. Typically, for 0.1 mM of Tl(I), Q_{Tl} is found to be 150, 122 and 50 $\mu C\,cm^{-2}$ at 0, 0.05 and 0.1 mM respectively of Pb(II). This indicates that at lower concentrations of lead, adatoms of lead do not cover the active sites on the silver surface completely, leaving enough sites for the formation of thallium adatoms. As Pb(II) is increased Q_{Pb} increases, consequently Q_{Tl} decreases. When Pb(II) exceeds 0.5 mM, a complete monolayer of lead is formed, leaving virtually no sites for thallium adatoms, which results in the absence of thallium UPD. This indicates that UPDs of lead and thallium are codeposited adjacent to each other and the formation of thallium UPD over the lead UPD layer is not likely. This is further seen from the facts that no reports of thallium UPD on lead are available from the literature, nor were efforts to obtain the thallium UPD on lead in the authors' laboratory successful.

Variation of Tl(I), keeping Pb(II) constant, has revealed the following. (i) At Tl(I) lower than 0.05 mM, the thallium UPD behaviour is distorted by diffusion limitations. (ii) In the range 0.05 mM to 0.5 mM, deposition and dissolution peaks of both lead and thallium UPDs are noticed, so long as Pb(II) does not exceed 0.1 mM. (iii) At Tl(I) higher than 0.5 mM, deposition peaks for both the UPDs are observed, but on the dissolution side only one peak corresponding to lead UPD alone is observed. This behaviour is also strongly influenced by the variation of sweep rate (cf. Section 3.2.2).

3.2.2. Effect of sweep rate. The variation of sweep rate is found to influence the codeposition behaviour of lead and thallium significantly. The deposition peak heights for the two UPDs vary in opposite directions with change in sweep rate (Fig. 2). At low sweep rates ($<0.02\,V\,s^{-1}$), deposition peaks for both UPDs are noticed, whereas on the dissolution side, a peak corresponding to lead is seen while that due to thallium is not observed except for a small hump of negligible charge at $0.01\,V\,s^{-1}$. Further, the charge due to lead UPD is found to be higher than that obtained for the dissolution of lead UPD resulting from lead solution (of identical concentration) alone under similar experimental conditions. With increase in sweep rate, a peak corresponding to thallium UPD appears, further increase in sweep rate resulting in increased coverage by thallium UPD and decrease in coverage by lead UPD. The charges corresponding to the lead and thallium dissolution peaks have been computed and presented in Fig. 3

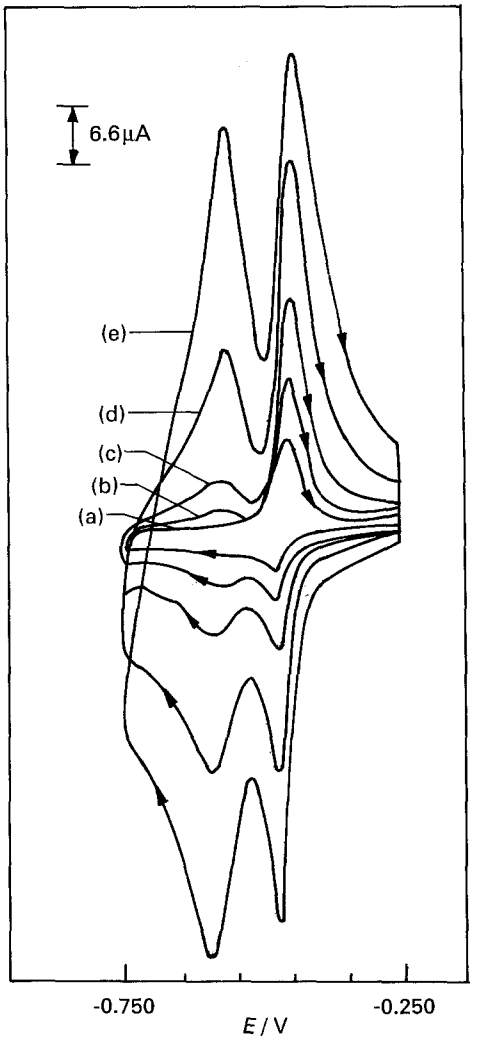

Fig. 2. Effect of sweep rate on CV response of polycrystalline silver from solution containing 5×10^{-5} M of Pb(II) and 10^{-4} M of Tl(I). Sweep rate: (a) 0.005, (b) 0.01, (c) 0.02, (d) 0.05 and (e) $0.1\,V\,s^{-1}$.

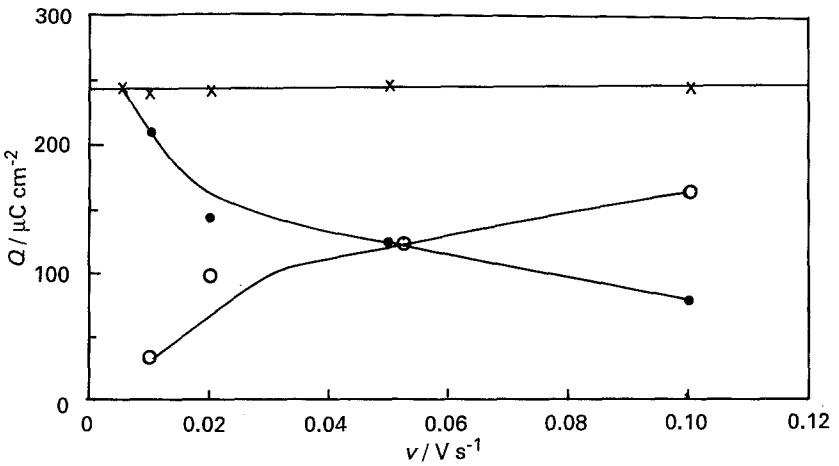

Fig. 3. Influence of sweep rate on the charge, Q, under the UPD peaks of lead and thallium (conditions are same as in Fig. 2). (—●—●) for Q_{Pb}, (—○—○) for Q_{Tl} and (—×—×) total charge $Q_{Pb} + Q_{Tl}$.

as a function of sweep rate. The total coverage due to lead and thallium is virtually constant ($250 \pm 20\,\mu C\,cm^{-2}$) over the range of sweep rates employed. This suggests that lead and thallium UPDs are formed on the silver substrate adjacent to each other. This is substantiated by experiments in which the potential sweep was held at UPD potential of lead (−0.46 V) for 5 min followed by a potential sweep continuing through the thallium region; this resulted in the disappearance of thallium UPD deposition and dissolution peaks which would otherwise be observable if preconcentration at −0.46 V was not effected.

A behaviour similar to the above is noticed when Pb(II) is increased to 0.1 mM except that the thallium UPD dissolution peak was seen only at sweep rates greater than $0.05\,V\,s^{-1}$ as against $0.02\,V\,s^{-1}$ observed for the lead concentration of 0.05 mM.

It can be deduced from the above results that: (i) lead and thallium UPDs occupy adjacent sites on the silver surface and do not grow over each other and (ii) at appropriate concentrations of Pb(II) and Tl(I) and at moderate sweep rates ($>0.05\,V\,s^{-1}$) both the deposition and dissolution peaks corresponding to the two UPDs are observed. Also, (iii), as against (ii), the use of higher Tl(I) at moderate sweep rates, or lower concentrations of thallium (<0.1 mM) at slower sweep rates ($<0.05\,V\,s^{-1}$) results in the formation of deposition peaks for both lead and thallium UPDs although only a single dissolution peak corresponding to lead UPD. However, the charge due to this single dissolution peak equals the sum of charges under the two deposition peaks (of Pb and Tl).

3.3. *Two-dimensional alloy from UPDs of Pb and Tl*

Realizing that there is no evidence for alloying between silver and lead and silver and thallium in the underpotential region [16, 21, 22], the merging of the individual anodic dissolution peaks of lead and thallium UPDs during codeposition (as in (iii) above) may be understood as follows. Thallium diffusion in lead is faster than the self-diffusion of lead [23]. Moreover, lead and thallium atoms possess a radius ratio that is favourable for the formation of a solid solution of Tl in lead (lead can dissolve about 87 at % of thallium [24]). So, it is reasonable to expect that the codeposited lead and thallium adatoms, if allowed to remain on the silver surface for sufficient time, can laterally coalesce resulting in the formation of a two-dimensional Pb–Tl alloy. This, upon anodic stripping yields a broad peak at potentials corresponding to the more electropositive metal, thereby indicating the alloy formed to be of solid solution type [25]. The crucial role of the time for 'coalescence' in the above alloy formation is borne out by the following experiments using the specially programmed potential sweep inputs (see insets of the Figs 4–6).

CVs recorded using different sweep rates for the forward and reverse scans are given in Fig. 4. Curve (a) depicts the behaviour recorded at the same sweep rate of $0.05\,V\,s^{-1}$ for both scans. Curve (b) at $0.005\,V\,s^{-1}$ for forward and $0.05\,V\,s^{-1}$ for reverse scans and curve (c) at $0.05\,V\,s^{-1}$ and $0.005\,V\,s^{-1}$ for cathodic and anodic scans, respectively. A decrease in the sweep rate of the cathodic scan results in changes of anodic charges of lead (Q_{Pb} increases) and thallium (Q_{Tl} decreases). Moreover, the loss in Q_{Tl} is almost equal to the gain in Q_{Pb}. These indicate that low cathodic sweep rates (i.e. large time scales) favour two-dimensional Pb–Tl UPD alloy formation.

In another set of experiments, the potential range corresponding to the deposition of thallium UPD alone (from −0.5 V to −0.7 V; see Fig. 5) is scanned at various sweep rates while the rest of the potential cycle is swept at $0.05\,V\,s^{-1}$. With decrease in sweep rate during thallium UPD deposition, the dissolution peak for thallium UPD decreases while that due to lead UPD increases. This again, supports the view that the formation of a two-dimensional solid solution type alloy from the lead and thallium UPDs is favoured at low sweep rates, i.e. at large time scales which facilitate coalescence between the two kinds of adatoms.

Confirmation of the above is provided in yet another set of experiments (cf. Fig. 6) in which the potential of the system was stepped to −0.7 V (covering the UPD region of Pb and Tl) and allowed to remain there for different time intervals (t_d) and then

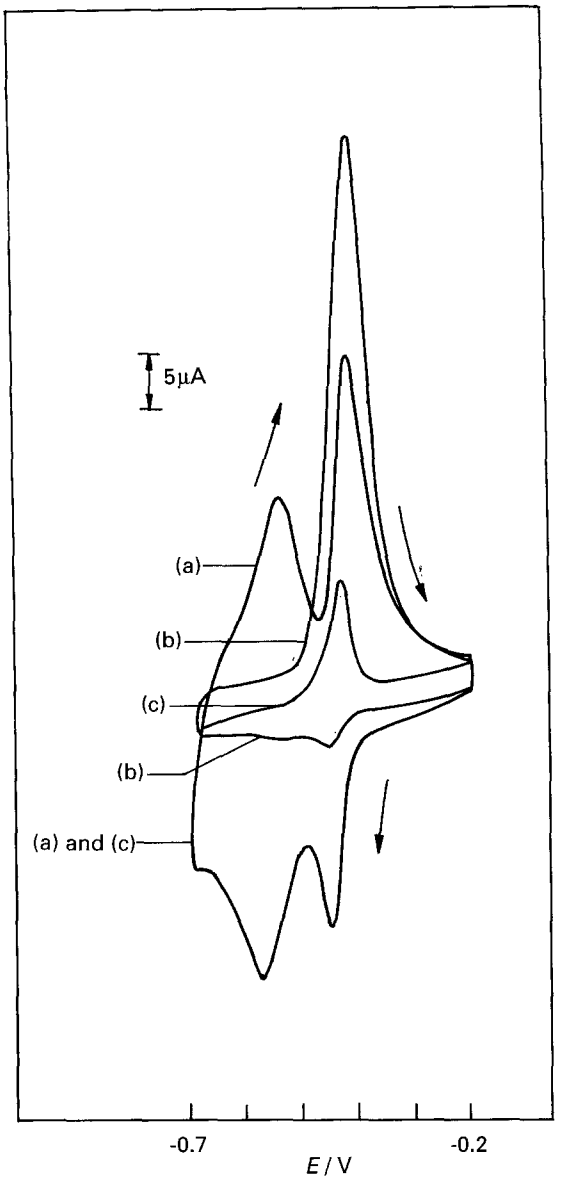

Fig. 4. Influence of the cathodic sweep rate on the dissolution pattern of the lead and thallium UPD in the anodic scan (a) 0.05 V s^{-1} for both cathodic and anodic sweeps, (b) 0.005 V s^{-1} for cathodic sweep and 0.05 V s^{-1} for anodic sweep and (c) 0.05 V s^{-1} for cathodic sweep and 0.005 V s^{-1} for anodic sweep.

stripped anodically at 0.05 V s^{-1}. With increase of t_d, the charge associated with thallium dissolution decreases while that of lead dissolution increases, and beyond a t_d value of 60 s, the thallium dissolution peak is completely absent, in accordance with the expectations based on two-dimensional alloy formation.

3.4. *Kinetic analysis of UPD*

The modelling of the formation and the growth of UPD has been extensively reported [26–32]. The model proposed by Bosco and Rangarajan [29] recognises the presence of both adsorption and nucleation processes and provides diagnostic criteria for analysing UPD systems under LSV conditions. Those criteria have been successfully employed in characterising several UPD systems [33–35]. Recently, we have demonstrated its application to a

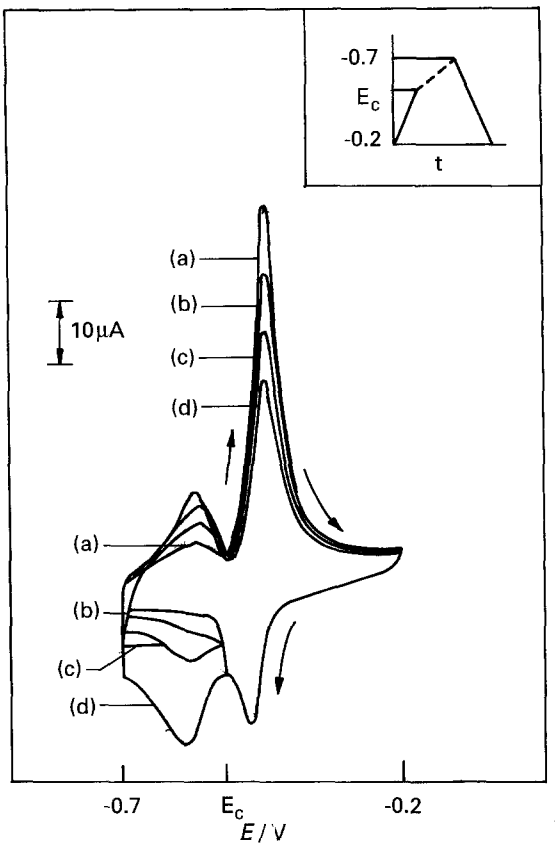

Fig. 5. Influence of sweep rate in the thallium UPD deposition range on the dissolution pattern of the lead and thallium UPD (sweep rate is varied only for the region from E_c to −0.7, while rest of the cycle is scanned at a sweep rate of 0.05 V s^{-1}). Sweep rate: (a) 0.005, (b) 0.01, (c) 0.02 and (d) 0.05 V s^{-1}.

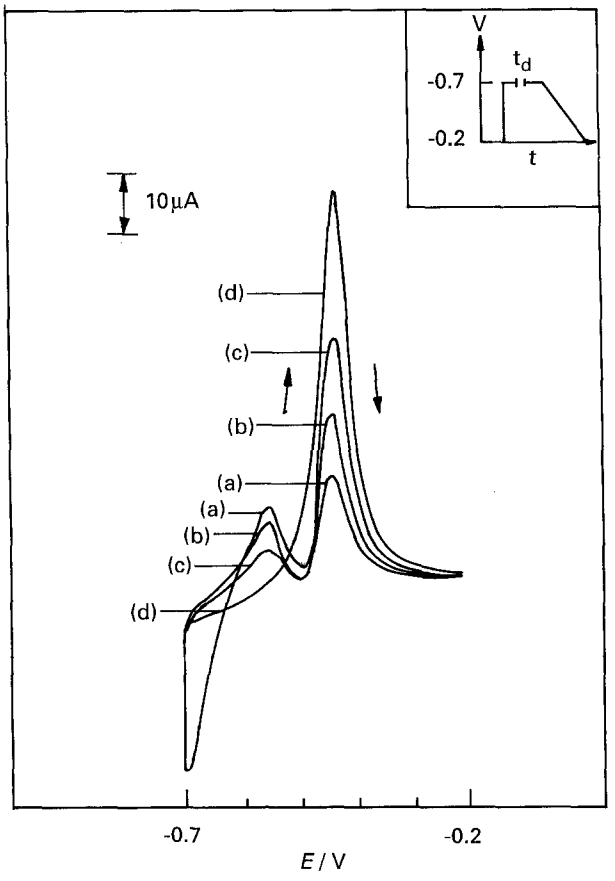

Fig. 6. Effect of 'holding time' (t_d) at −0.7 V on the dissolution pattern of lead and thallium UPD region. t_d: (a) 0, (b) 10, (c) 25 and (d) 60 s. Sweep rate employed for stripping is 0.05 V s^{-1}.

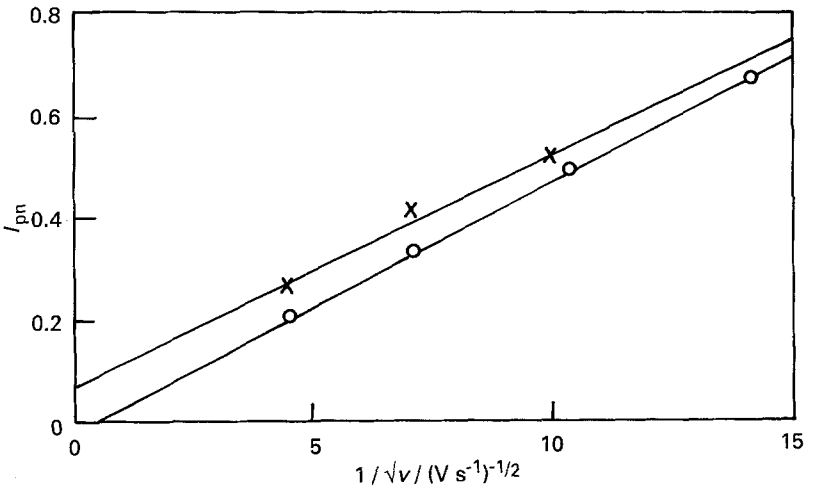

Fig. 7. Plots of I_{pn} against $1/\sqrt{v}$ for lead UPD from solution containing (i) (×—×) Pb(II) alone and (ii) (○—○) Pb(II) and Tl(I).

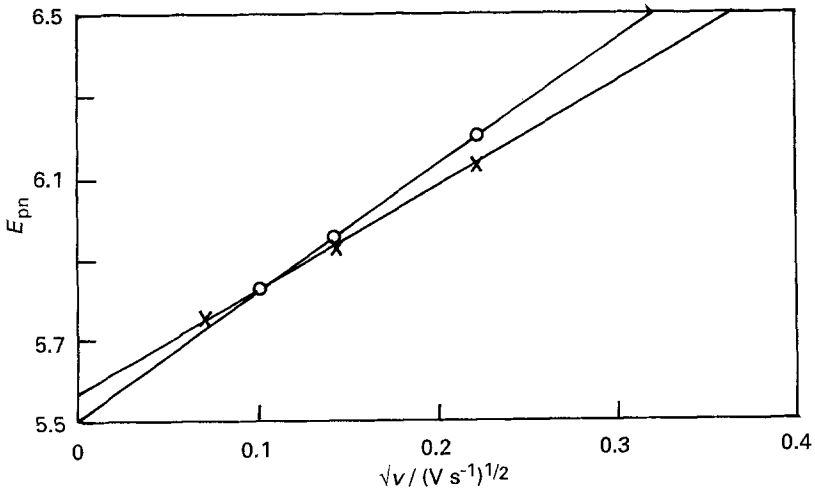

Fig. 8. Plots of E_{pn} against $\sqrt{v}$ for lead UPD from solution containing (i) (○—○) Pb(II) alone and (ii) (×—×) Pb(II) and Tl(I).

mixed UPD system [16]. The present system, when subjected to similar analysis using Bosco and Rangarajan modelling, yielded the following results. Linear relationship resulting from the plots of (i) I_{pn} against $1/\sqrt{v}$ (Fig. 7), (ii) E_{pn} against $\sqrt{v}$ (Fig. 8) and (iii) $\Delta E_{\frac{1}{2}n}$ against $\sqrt{v}$ (Fig. 9) for lead UPD both when lead is present alone and along with thallium UPD suggests a nucleation growth process. Additionally, the linear plot of I_{pn} against $1/E_{pn}$ (Fig. 10) characterizes the growth to be under instantaneous nucleation control. Staikov *et al.* [19] have noted that the citrate anions form a preadsorbed layer on silver and lead UPD proceeds through a nucleative mechanism.

The slopes of the linear plots f I_{pn} against $1/\sqrt{v}$, E_{pn} against $\sqrt{v}$ and $\Delta E_{\frac{1}{2}n}$ against $\sqrt{v}$ given by I, II and III, respectively, below [30]:

$$(2.3)^{3/4}(\sqrt{\beta}4RT/zF)^{1/2} \quad \text{(I)}$$

$$(3)^{1/4}(\sqrt{\beta}4RT/zF)^{-1/2} \quad \text{(II)}$$

$$(1.22/4^{3/4})(\sqrt{\beta}4RT/zF)^{-1/2} \quad \text{(III)}$$

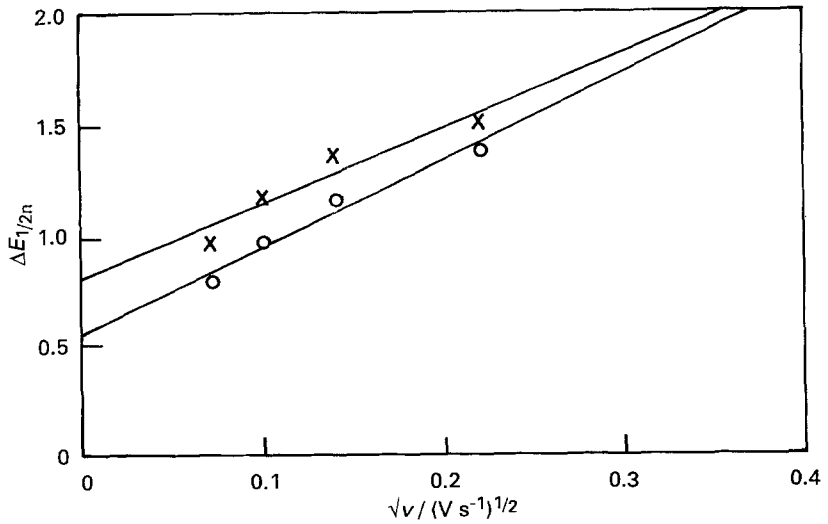

Fig. 9. Plots of $\Delta E_{\frac{1}{2}n}$ against $\sqrt{v}$ for lead UPD from solution containing (i) (×—×) Pb(II) alone and (ii) (○—○) Pb(II) and Tl(I).

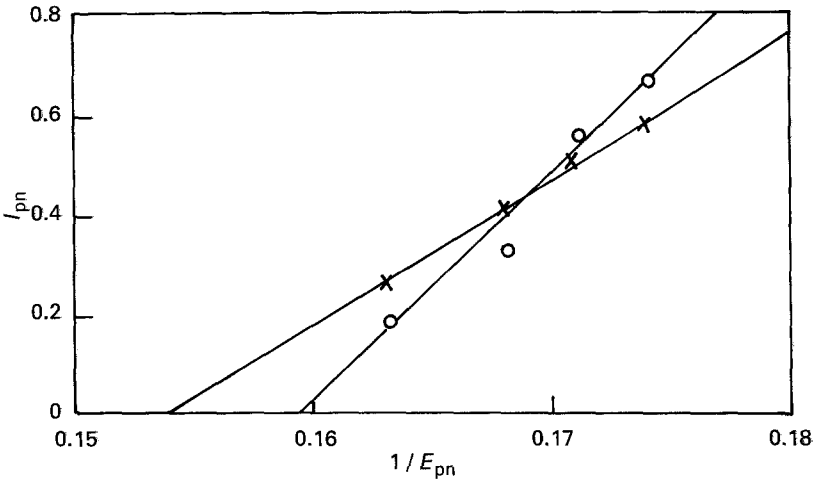

Fig. 10. Plots of I_{pn} against $1/E_{pn}$ for lead UPD from solution containing (i) (—×—×) Pb(II) alone and (ii) (—○—○) Pb(II) and Tl(I).

allowed computation of the instantaneous nucleation growth rate constants (β) from three different routes. The β values calculated for the lead UPD from Pb(II) solutions, both in the presence and the absence of Tl(I), are presented in Table 2, which shows that β values from the three different routes agree closely. Further, these β values derived for the tartrate medium are about one order of magnitude less than those obtained in citrate (cf. in citrate $\beta \approx 10^1$ [17]).

Table 2. Instantaneous nucleation rate constant β [30] calculated for Pb UPD from tartrate and citrate [17] media containing (i) Pb(II) alone and (ii) Pb(II) and Tl(I)

Method	*Tartrate*		*Citrate*	
	(i)	*(ii)*	*(i)*	*(ii)*
I_{pn} against $1\sqrt{v}$	0.50	0.34	25.0	12.0
E_{pn} against $\sqrt{v}$	0.42	0.32	76.0	10.7
$\Delta E_{\frac{1}{2}n}$ against $\sqrt{v}$	0.21	0.17	22.8	18.0

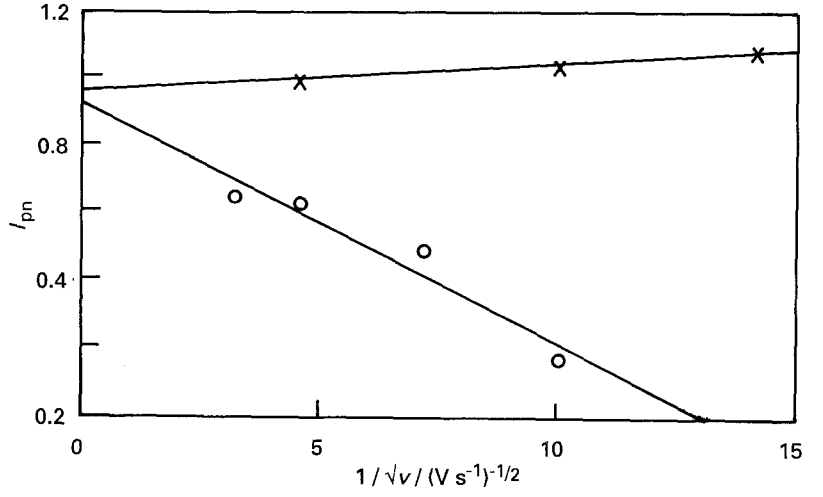

Fig. 11. Plots of I_{pn} against $1/\sqrt{v}$ for thallium UPD from solution containing (i) (—×—×) Tl(I) alone and (ii) (—○—○) Tl(I) and Pb(II).

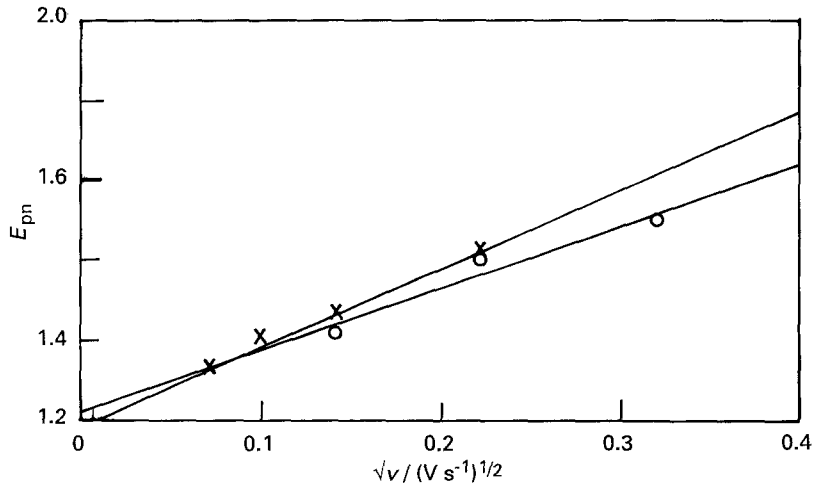

Fig. 12. Plots of E_{pn} against $\sqrt{v}$ for thallium UPD from solution containing (i) (—×—×) Tl(I) alone and (ii) (—○—○) Tl(I) and Pb(II).

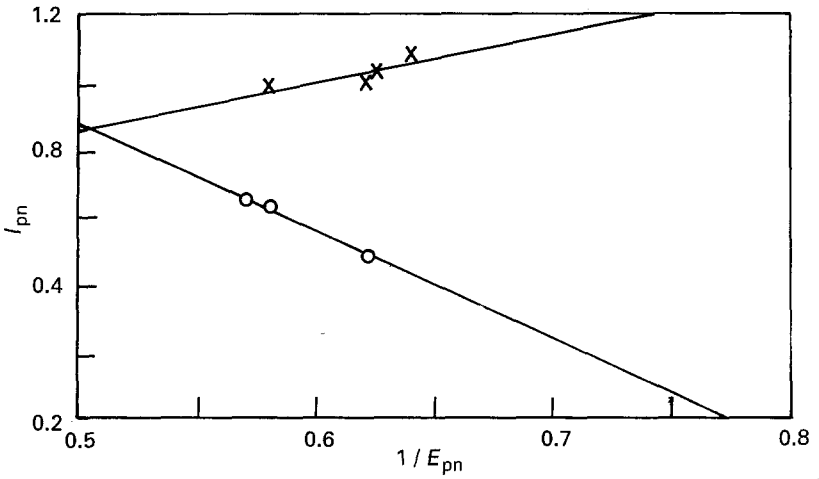

Fig. 13. Plots of I_{pn} against $1/E_{pn}$ for thallium UPD from solution containing (i) (—×—×) Tl(I) alone and (ii) (—○—○) Tl(I) and Pb(II).

Similarly, the data for the individual thallium UPD, when analysed using the above diagnostic criteria, resulted in linear plots for (i) I_{pn} against $1/\sqrt{v}$ (Fig. 11), (ii) E_{pn} against $\sqrt{v}$ (Fig. 12) and (iii) $\Delta E_{\frac{1}{2}n}$ against $\sqrt{v}$ (Fig. 13), thereby indicating nucleation-growth kinetics.

However, the formation of thallium UPD during codeposition defies the criteria for both nucleation and adsorption models. This is possibly due to thallium UPD, during codeposition, taking place on the silver surface which is partially covered with lead UPD (unlike the case of lead UPD formation during codeposition).

4. Conclusions

Simultaneous UPD of lead and thallium on polycrystalline silver from tartrate medium has been achieved through a codeposition approach. The adatoms of lead and thallium grow adjacent to each other and, if allowed to remain on the silver surface for sufficient time, coalesce to form a two-dimensional solid solution type alloy. The growth of lead and thallium UPDs individually and the lead UPD during codeposition from the tartrate medium follows nucleation kinetics.

Acknowledgements

One of the authors (SB) thanks CSIR, India for the award of Senior Research Fellowship.

References

[1] D. M. Kolb, *in* 'Advances in Electrochemistry and Electrochemical Engineering' Vol. 11 (edited by H. Gerischer and C. W. Tobias) Wiley, New York (1978).
[2] R. R. Adzic, *in* 'Advances in Electrochemistry and Electrochemical Engineering' Vol. 13 (edited by H. Gerischer and C. W. Tobias) Wiley, New York (1984).
[3] Z. Szoba, *Int. Reviews Phys. Chem.* **10** (1991) 207.
[4] G. Kokinidis, *J. Electroanal. Chem.* **201** (1986) 217.
[5] K. Juttner, *Electrochim. Acta* **31** (1986) 917.
[6] A. R. Despic *in* 'Electrode Processes', ECS Symposium Series Vol. 80-3, (1979) p. 235.
[7] D. C. Alonzo and B. R. Scharifker, *J. Electroanal. Chem.* **274** (1989) 167.
[8] E. Schmidt and H. R. Gygax, *Helv. Chim. Acta* **49** (1966) 1105.
[9] G. W. Tindall and S. Bruckenstein, *J. Electroanal. Chem.* **22** (1965) 295.
[10] S. Stucki, *J. Electroanal. Chem.* **78** (1977) 31.
[11] K. Juttner and H. J. Pauling, *B. Electrochem.* **8** (1992) 62.
[12] H. J. Pauling and K. Juttner, *Electrochim. Acta* **37** (1992) 2237.
[13] H. J. Pauling, I. H. Omar and K. Juttner, *Metalloberflache* **47** (1993) 66.
[14] S. Bharathi, V. Yegnaraman and G. Prabhakara Rao, *B. Electrochem.* **6** (1990) 658.
[15] *Idem, Appl. Surf. Science* **47** (1991) 293.
[16] *Idem, Electrochim. Acta* **36** (1991) 1291.
[17] D. M. Kolb, M. Przasnyski and H. Gerischer, *J. Electroanal. Chem.* **54** (1974) 25.
[18] G. Staikov, K. Juttner, W. J. Lorenz and E. Schmidt, *Electrochim. Acta* **23** (1978) 305.
[19] S. Bharathi, PhD dissertation (1992) Alagappa University, India.
[20] J. H. White and H. D. Abruna, *J. Phys. Chem.* **94** (1990) 894.
[21] H. Seigenthaler and K. Juttner, *Electrochim. Acta* **24** (1979) 109.
[22] *Idem, ibid.* **23** (1978) 971.
[23] W. K. Waburton and D. Turnbull, *in* 'Diffusion in Solids: Recent Developments' (Edited by A. S. Nowick and J. J. Burton) Academic Press, New York (1974).
[24] W. B. Pearson, 'A Handbook of Lattice Spacings and Structures of Metals and Alloys', Pergamon, London (1958).
[25] S. Swathirajan, *J. Electrochem. Soc.* **133** (1986) 671.
[26] S. Srinivasan and E. Gileadi, *Electrochim. Acta* **11** (1966) 321.
[27] H. Angerstein-Kozlowska, J. Klinger and B. E. Conway, *J. Electroanal. Chem.* **75** (1977) 45.
[28] *Idem, ibid.* **87** (1978) 301.
[29] E. Bosco and S. K. Rangarajan, *ibid.* **129** (1981) 25.
[30] E. Bosco and S. K. Rangarajan, *J. Chem. Soc., Faraday Trans. I* **77** (1981) 1679.
[31] M. Noel, S. Chandrasekaran and C. A. Basha, *J. Electroanal. Chem.* **225** (1987) 93.
[32] A. Bewick and B. Thomas, *ibid.* **65** (1975) 911.
[33] S. Jaya, T. Prasada Rao and G. Prabhakara Rao, *Electrochim. Acta.* **31** (1986) 343.
[34] *Idem, ibid.* **31** (1986) 1601.
[35] *Idem, ibid.* **32** (1987) 1073.